THE JOURNAL OF BIOLOGICAL CHEMISTRY Vol. 280, No. 2, Issue of January 14, pp. 1603–1612, 2005

Printed in U.S.A.

The Conserved Immunoglobulin Domain Controls the Subcellular Localization of the Homophilic Adhesion Receptor Protein-tyrosine Phosphatase μ*

Received for publication, September 3, 2004, and in revised form, October 13, 2004
Published, JBC Papers in Press, October 18, 2004, DOI 10.1074/jbc.M410181200

Robert L. Del Vecchio and Nicholas K. Tonks‡

From the Cold Spring Harbor Laboratory, Cold Spring Harbor, New York 11724

The receptor protein-tyrosine phosphatase μ (PTPμ) is a homophilic adhesion protein thought to regulate cell-cell adhesion in the vascular endothelium through dephosphorylation of cell junction proteins. In subconfluent cell cultures, PTPμ resides in an intracellular membrane pool; however, as culture density increases and cell contacts form, the phosphatase localizes to sites of cell-cell contact, and its expression level increases. These characteristics of PTPμ, which are consistent with a role in cell-cell adhesion, suggest that control of subcellular localization is an important mechanism to regulate the function of this phosphatase. To gain a better understanding of how PTPμ is regulated, we examined the importance of the conserved immunoglobulin domain, containing the homophilic binding site, in control of the localization of the enzyme. Deletion of the immunoglobulin domain impaired localization of PTPμ to the cell-cell contacts in endothelial and epithelial cells. In addition, deletion of the immunoglobulin domain affected the distribution of PTPμ in subconfluent endothelial cells when homophilic binding to another PTPμ molecule on an apposing cell was not possible, resulting in an accumulation of the mutant phosphatase at the cell surface with a concentration at the cell periphery in the region occupied by focal adhesions. This aberrant localization correlated with reduced survival and alterations in normal focal adhesion and cytoskeleton morphology. This study therefore illustrates the critical role of the immunoglobulin domain in regulation of the localization of PTPμ and the importance of such control for the maintenance of normal cell physiology.

The physical interactions of individual cells with the local environment is critical to the control of their growth, differentiation, and fate within a multicellular organism. These responses are initiated by cell adhesion receptors, which bind either homophilic or heterophilic ligands on apposing cells or the extracellular matrix. A critical aspect in the cellular response to these interactions is reversible protein tyrosine phosphorylation of cell junction-associated proteins (1, 2). In fact, the bulk of the tyrosine-phosphorylated cellular proteins are localized to sites of cell-cell and cell-extracellular matrix adhesion. Several protein-tyrosine kinases and phosphatases have been implicated in the regulation of cell adhesion (3–6). In particular, receptor protein-tyrosine phosphatases (RPTPs),[1] several of which possess extracellular domains with features characteristic of cell adhesion receptors, linked to a cytoplasmic PTP activity, are uniquely designed to mediate cellular responses to adhesive signals through protein tyrosine dephosphorylation (7, 8). Of particular interest is the potential for the extracellular domains of individual RPTPs to mediate interactions with, and control of, either cell-cell or cell-extracellular matrix adhesions. In this way, the targeting of RPTPs to specific junctions may be a key element in controlling the changes in cell junction-actin cytoskeleton interactions that occur as cells transition from a growing, migrating state, in which actin stress fibers are linked to cell-matrix junctions, to contact-inhibited cells, in which actin fibers are linked primarily to cell-cell junctions (9).

In this study, we focus on the receptor protein-tyrosine phosphatase PTPμ. PTPμ is synthesized as a single polypeptide chain, which is then glycosylated and proteolytically cleaved at a site N-terminal to the transmembrane segment to give two subunits that remain noncovalently associated (10, 11). The E-subunit (see Fig. 1*A*), which constitutes the majority of the extracellular segment, consists of one immunoglobulin (Ig) domain; four fibronectin type III repeats; and a MAM (Mu, A5, and meprin homology) domain, which is a conserved domain unique to PTPμ, PTPκ, PTPρ, and PTPλ and some cell adhesion molecules (12). The P-subunit (see Fig. 1*A*) contains a short extracellular segment; the transmembrane segment; and the entire cytoplasmic portion, including two PTP domains. PTPμ can function as a homophilic adhesion receptor whereby a PTPμ molecule on one cell can bind to an identical PTPμ molecule on an apposing cell (13, 14). It is this binding that is proposed to direct the localization of PTPμ to sites of cell-cell contact, where it is thought to interact with the cadherin-catenin cell adhesion complex (11, 15). Consistent with a role in cell-cell adhesion, the level of PTPμ protein increases as intercellular contacts are made and cell-cell junctions form (11). This phenomenon is seen with other RPTPs and may provide a means to control protein phosphotyrosine-based signaling in contact-inhibited cells (15–18). PTPμ is expressed predominantly in vascular endothelial cells and to a lesser extent in bronchial epithelium and may play a role in endothelium-dependent processes such as the control of vascular permeability and the angiogenic responses to tumor formation and wound healing (19).

* This work was supported by National Institutes of Health Grant GM55989. The costs of publication of this article were defrayed in part by the payment of page charges. This article must therefore be hereby marked "*advertisement*" in accordance with 18 U.S.C. Section 1734 solely to indicate this fact.

‡ To whom correspondence should be addressed: Cold Spring Harbor Lab., 1 Bungtown Rd., Cold Spring Harbor, NY 11724. Tel.: 516-367-8846; Fax: 516-367-6812; E-mail: tonks@cshl.edu.

[1] The abbreviations used are: RPTPs, receptor protein-tyrosine phosphatases; PTP, protein-tyrosine phosphatase; BAEC, bovine aortic endothelial cells; trBAEC, transformed bovine aortic endothelial cells; MDCK, Madin-Darby canine kidney; BrdUrd, 5-bromo-2-deoxyuridine; WT, wild-type; Ig, immunoglobulin; MEM, minimum essential media; VE-cadherin, vascular endothelial cadherin.

Considering the importance of PTPs in the control of signal transduction, it is critical that they be tightly regulated to facilitate protein tyrosine phosphorylation (20). Based on studies with RPTPα, dimerization of RPTPs, which leads to occlusion of the active site, has been proposed as one mechanism for inhibition of phosphatase activity (21–23). However, it is not clear whether dimer-induced inhibition is widely applicable, as dimers formed in crystals of RPTP-LAR and RPTPμ are oriented such that the active sites are unobstructed (24, 25). A number of studies indicate that the control of localization and substrate accessibility by intrinsic targeting domains is another important way to modulate cellular dephosphorylation by PTPs (20) such as PTPμ. In contrast to the structurally related LAR-subtype RPTPs (LAR, PTPσ, and PTPδ), which can be found in both cell-matrix and cell-cell contacts (26–28), PTPμ is thought to function exclusively at sites of cell-cell adhesion, where it has the potential to regulate signaling events specific to contact-inhibited cells. In subconfluent cells, PTPμ is thought to cycle between the plasma membrane and membrane vesicles in the perinuclear region of the cell (11, 15). Although it has been proposed that stable surface expression is dependent upon homophilic binding at cell-cell contacts (11), the mechanism whereby PTPμ localization is controlled has not been defined.

Previous studies using purified fusion proteins indicate that the conserved Ig domain is necessary and sufficient for homophilic binding of purified PTPμ fusion proteins as well as binding of the fusion proteins to the surface of cells expressing endogenous levels of PTPμ (10). Here, we have deleted the Ig domain of PTPμ and expressed the mutant protein in endothelial and epithelial cell lines to assess the role of this domain in regulating localization of the phosphatase. The results demonstrate the importance of the Ig domain for the localization of PTPμ to sites of cell-cell contact and also identify a role for this domain in localization of PTPμ in subconfluent cells in the absence of cell-cell contact.

EXPERIMENTAL PROCEDURES

Cell Culture—Bovine aortic endothelial cells (BAEC) and the derived cell lines GM7372 and GM7373 (referred to here as transformed BAEC (trBAEC)) (29) were obtained from the Coriell Institute for Medical Research (Camden, NJ). The cells were grown in basal medium (Sigma) supplemented with 10% fetal bovine serum (Hyclone Laboratories), 1× MEM/essential and nonessential amino acid mixtures, 1× MEM/vitamin mixture, 2 mM L-glutamine, and 10 μg/ml gentamycin (Invitrogen). Madin-Darby canine kidney (MDCK) cells (catalog no. CCL-34) were purchased from American Type Culture Collection (Manassas, VA) and grown in Dulbecco's modified Eagle's medium (Invitrogen) plus 10% fetal bovine serum, 2 mM L-glutamine, and 10 μg/ml gentamycin.

Construction of Retroviral Expression Plasmids—Human PTPμ (GenBank™/EBI accession number NM_002845) DNA constructs were cloned with a C-terminal T7 epitope tag (30) into the retroviral vector pWZL-hygro (provided by S. Lowe, Cold Spring Harbor Laboratory) by PCR with pBSK/hFL (31) as the template. pWZL/PTPμWT contains nucleotides 1–4359 of human PTPμ; pWZL/PTPμΔIg and pWZL/PTPμΔE have deletions of nucleotides 568–930 and 67–1914, respectively, in human PTPμ. The resulting constructs encoded proteins with a C-terminal extension of AGMASMTGGQQMG, where the underlined amino acids define the T7 epitope tag. All constructs derived from PCR were confirmed by DNA sequencing.

Expression of PTPμ by Retroviral Infection—LiNX-A retroviral packaging cells (32) were transfected with pWZL/PTPμ plasmid DNA using calcium phosphate. The resulting supernatants, containing recombinant retrovirus encoding PTPμ, were used to infect monolayer cultures of GM7372 cells, trBAEC, or MDCK cells. Two days following infection, cells were placed in the appropriate medium supplemented with 100 μg/ml (GM7372 cells) or 400 μg/ml (trBAEC and MDCK cells) hygromycin B (Invitrogen). The medium was changed every 2–3 days, and cultures were passaged when they reached ~70–90% confluence.

Antibodies—The following primary antibodies were used in this study: anti-T7 epitope antibody (mouse IgG2b; Novagen); anti-VE-cadherin antibody 45C6 (mouse IgG1; ICOS, Bothell, WA); anti-vinculin antibody VIN-11-5 (mouse IgG1; Sigma); anti-phosphotyrosine antibody G104 (mouse IgG1) (33); anti-paxillin antibody (mouse IgG1; Transduction Laboratories); and the PTPμ-specific antibodies SK7 (mouse IgG1), BK2 (mouse IgG2a), and BK3 (mouse IgG1) (15).

Indirect Immunofluorescence—Cells were plated on glass coverslips, grown to the desired density, and fixed with 2% paraformaldehyde in phosphate-buffered saline for 12.5 min. Cells were either permeabilized in phosphate-buffered saline, 3% normal goat serum, and 0.2% Triton X-100 for 20 min or left intact as indicated. Fixed samples were incubated either with single primary antibodies or, for co-staining, with two antibodies of different isotypes. The primary antibodies were detected with isotype-specific secondary antibodies (Molecular Probes, Inc., Eugene, OR) to mouse IgG1 (labeled with Alexa 594) or to mouse IgG2b or IgG2a (labeled with Alexa 488).

Co-staining with antibodies SK7 and 45C6, both of which are IgG1 isotype, was performed as follows. Fixed cells were first incubated with antibody SK7, followed by a 20-fold excess of Fab fragments of rabbit anti-mouse IgG and then Texas Red-labeled anti-rabbit IgG. Then the cells were incubated with antibody 45C6, followed by fluorescein isothiocyanate-labeled rabbit anti-mouse IgG. A control sample in which antibody 45C6 was omitted did not show staining with the fluorescein isothiocyanate-labeled anti-mouse IgG, indicating that the excess, Fab fragment rabbit anti-mouse IgG, effectively blocked antibody SK7 from reaction with this secondary antibody.

Coverslips were mounted on glass slides using ProLong anti-fade reagent (Molecular Probes, Inc.) and examined by epifluorescence using an Axiophot 2 microscope and digital imaging system with a ×63 objective lens (Carl Zeiss Microimaging, Thornwood, NY) unless indicated otherwise. Images were processed using OpenLab software (Improvision Software, Lexington, MA). Confocal images were obtained with a Zeiss LSM510 confocal microscopy system using a ×100 objective lens and processed with built-in software and ImageJ software (National Institute of Mental Health, available at rsb.info.nih.gov/ij/).

Immunoblotting and Immunoprecipitation—GM7372 cells were grown to the desired density and solubilized in lysis buffer (30 mM HEPES (pH 7.5), 150 mM NaCl, 1% Triton X-100, 8% glycerol, 1 mM EDTA, 1 mM benzamidine, and 5 μg/ml each aprotinin and leupeptin) for 30 min. Lysates were centrifuged at 10,000 × *g* for 15 min, and the resulting supernatants were assayed for protein concentration with Bradford reagent using bovine serum albumin as the standard. Equal amounts of protein were separated by SDS-PAGE and transferred to nitrocellulose membranes for immunoblotting with anti-PTPμ monoclonal antibodies SK7 and BK2 as described (15). For immunoprecipitations, equal amounts of protein from GM7372 cell lysates, prepared as described above, were incubated with anti-T7 epitope antibody-conjugated agarose (Novagen) for 2 h at 4 °C. Samples were washed four times in lysis buffer, and bound proteins were eluted with Laemmli sample buffer, separated by SDS-PAGE, and analyzed by immunoblotting.

Assay of Cell Proliferation and Apoptosis—Proliferation rates of cell lines were assayed by measuring incorporation of 5-bromo-2-deoxyuridine (BrdUrd). Cells were plated on glass coverslips at a density of 4×10^3 cells/cm^2, and 36 h later, 20 μM BrdUrd was added for 40 min. Cells were stained for BrdUrd incorporation using fluorescein isothiocyanate-conjugated anti-BrdUrd antibody (Roche Applied Science) according to the manufacturer's protocol. Samples were co-stained with Hoechst 33342 (Molecular Probes, Inc.) to visualize nuclei of all cells and imaged by epifluorescence using a ×10 objective. Total and BrdUrd-positive cells were counted in images using ImageJ software, and the percentage of BrdUrd-positive cells was calculated.

To assay for apoptosis, cells were plated on glass coverslips at 4×10^3 cells/cm^2 and incubated at 37 °C for 36 h. Cells were fixed as described above for immunofluorescence and stained with Hoechst 33342 according to the supplier's protocol. Cells displaying condensed chromatin and the formation of nuclear blebs containing DNA were counted as apoptotic. The percentage of apoptotic cells in six representative fields of each sample was calculated as described above for the assay of BrdUrd incorporation.

RESULTS

Generation of Stable Lines of GM7372 Cells Expressing PTPμ Deletion Constructs—As an initial step in understanding the mechanisms involved in regulating PTPμ function in endothelial cells, we expressed various mutant constructs in GM7372 cells, a cell line derived from BAEC. GM7372 cells have similar morphology and growth properties compared with primary BAEC and express endothelium-specific cell junction

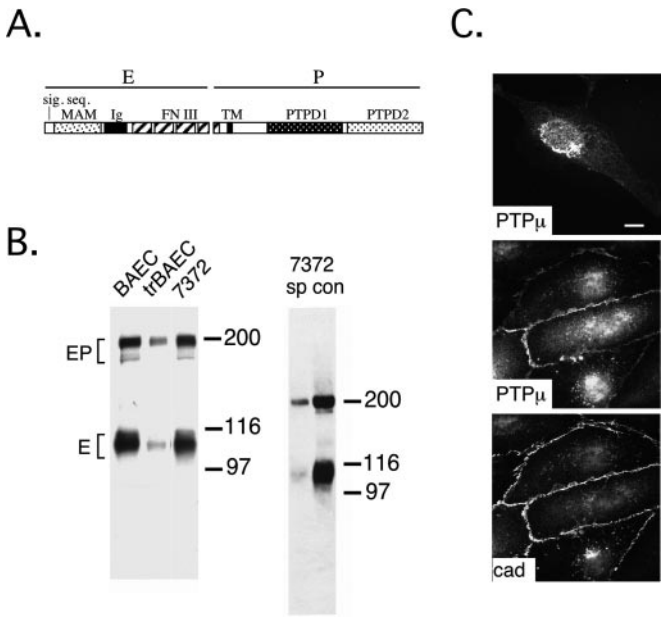

FIG. 1. **Endogenous PTPμ expression in bovine endothelial cells.** *A*, the domain structure of PTPμ is outlined with the signal sequence (*sig. seq.*) and the MAM, immunoglobulin (Ig), fibronectin type III repeat (*FN III*), transmembrane (*TM*), and tandem catalytic (*PTPD1/D2*) domains indicated above the diagram. The positions of the E- and P-subunits (amino acids 23–638 and 639–1452, respectively) are indicated. *B*, lysates from confluent cultures of BAEC, trBAEC, and GM7372 cells (*7372*) (*left panel*) and sparse (*sp*; ~40% confluent) and confluent (*con*) GM7372 cells (*right panel*) were analyzed by immunoblotting with anti-PTPμ antibody BK2. 40 μg of protein were loaded for each lysate. *Brackets* indicate the positions of the non-proteolytically processed protein (*EP*) and the proteolytically processed E-subunit (*E*). Pulse-chase labeling studies suggested that the lower band(s) for the EP protein represents the initial protein product prior to glycosylation and subsequent processing. The migration positions of relative molecular mass markers (in kilodaltons) are shown to the right of each panel. *C*, subconfluent GM7372 cells were fixed and stained with anti-PTPμ antibody SK7 (*upper panel*), and confluent cells were stained sequentially with antibody SK7 (*middle panel*) and anti-VE-cadherin antibody 45C6 (*cad*; *lower panel*) as described under "Experimental Procedures." *Scale bar* = 10 μm.

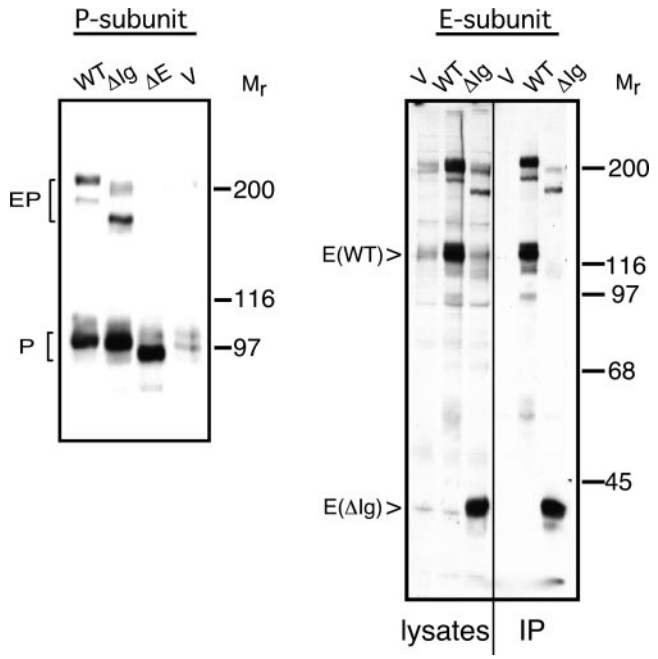

FIG. 2. **Analysis of PTPμ proteins expressed in GM7372 cells.** Lysates from stable populations of confluent GM7372 cells expressing PTPμWT, PTPμΔIg, PTPμΔE, or the empty pWZL-hygro vector (*V*) were analyzed by immunoblotting with anti-P-subunit antibody SK7 (*left panel*) or anti-E-subunit antibody BK2 (*right panel*, *lysate lanes*). 18 μg of protein were loaded for each lysate. Immunoblotting conditions were chosen to demonstrate the overexpression of the ectopic proteins relative to endogenous PTPμ. The positions of the non-proteolytically processed protein (*EP*) and the processed P-subunit (*P*) and E-subunits of the PTPμWT (*E(WT)*) and PTPμΔIg (*E(ΔIg)*) proteins are indicated to the left of the panels. Pulse-chase labeling studies suggested that the lower band(s) for the EP protein represents the initial protein product prior to glycosylation and subsequent processing. The band at 116 kDa in the PTPμΔIg samples, which also appears in the vector samples, is from the endogenous PTPμ E-subunit. Association of the two subunits of PTPμWT or PTPμΔIg was demonstrated by immunoprecipitating the P-subunit from lysates of GM7372 cells with the anti-T7 epitope antibody and detecting the associated E-subunit by immunoblotting the immune complexes with antibody BK3 (*right panel*, *IP lanes*). The migration positions of the E-subunits from the PTPμWT and PTPμΔIg proteins are indicated to the left of the *right panel*. The migration positions of relative molecular mass markers (in kilodaltons) are indicated to the right of each panel.

proteins (Fig. 1) (data not shown) (29). GM7372 cells expressed a similar level of endogenous PTPμ compared with the parental BAEC (Fig. 1*B*). In agreement with previous findings (15, 19), PTPμ was observed as a full-length ~200 kDa protein (Fig. 1*B*, *EP*) and as processed proteolytic fragments of ~110 kDa for the E-subunit (Fig. 1*B*, *E*) and P-subunit (data not shown). As described previously (19), at high cell density, PTPμ co-localized at cell-cell contacts with the endothelial-specific VE-cadherin, and the level of PTPμ protein was increased (Fig. 1, *B* and *C*). In subconfluent cells, PTPμ was found in a perinuclear vesicular compartment (Fig. 1*C*).

Ectopic expression of PTPμWT, PTPμΔIg (deletion of amino acids 190–310), and PTPμΔE (deletion of amino acids 23–638) was achieved by infection of GM7372 monolayers with recombinant retrovirus encoding the T7 epitope-tagged PTPμ constructs. We utilized a vector, pWZL, containing an internal ribosomal entry site, from which PTPμ and the selection marker are separately translated from the same mRNA. Stable cells were selected in hygromycin as pooled populations from an ~90% confluent monolayer of infected GM7372 cells. Attempts to isolate clonal cell lines of GM7372 expressing PTPμ from dilute cultures were unsuccessful. We reasoned that any inhibitory effects on growth or survival caused by ectopic expression of PTPμ might be more pronounced at low cell density, when the normal level of PTPμ is low, than at high cell density, when expression of the phosphatase is naturally up-regulated. The use of the pWZL vector resulted in a tight correlation between hygromycin resistance and ectopic expression of PTPμ, producing cell populations in which 70–80% of the cells expressed detectable amounts of the specific PTPμ mutant, as determined by detection with anti-PTPμ antibodies (data not shown).

Immunoblotting of cell lysates with antibodies specific to the P-subunit (SK7) and the E-subunit (BK2) indicated similar levels of expression from each construct (Fig. 2). Furthermore, the wild-type EP protein migrated as a doublet on SDS-polyacrylamide gel, with the slower migrating band, previously shown to represent the glycosylated form (11), predominating. In contrast, the hypoglycosylated form of PTPμΔIg predominated, which would contribute to the faster than expected migration of the E-subunit of this mutant on SDS-polyacrylamide gel. In addition, immunoprecipitation of the P-subunit of PTPμΔIg with the antibody to the C-terminal T7 epitope followed by immunoblotting of the E-subunit with antibody BK3 demonstrated that the two intact segments of the processed protein were associated in the cell, as seen with the WT protein (Fig. 2).

The Ig Domain Is the Major Determinant of Localization of PTPμ to Sites of Cell-Cell Contact—It has been proposed that

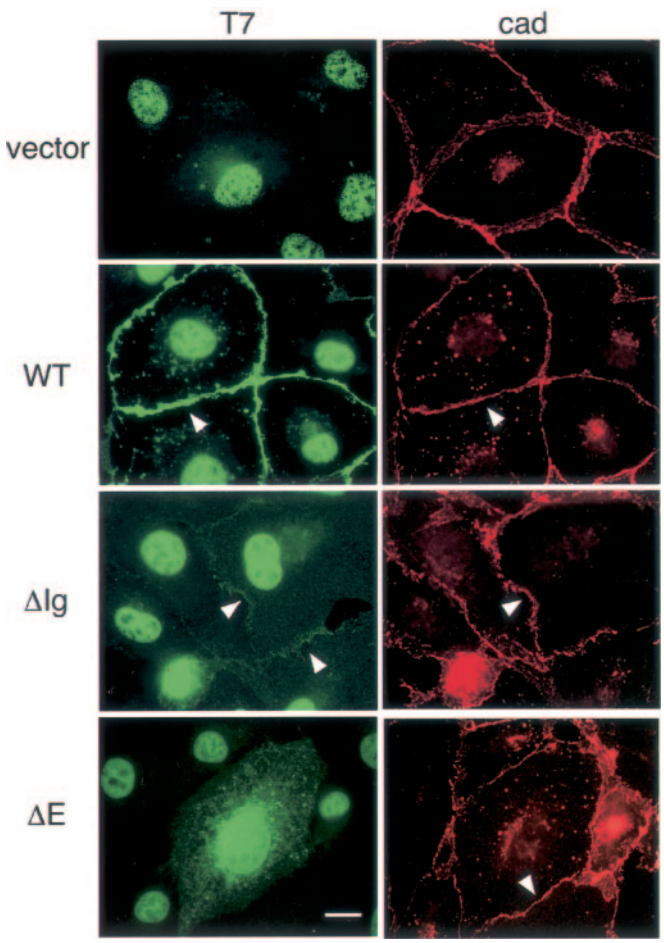

FIG. 3. **Deletion of the Ig domain reduces localization of PTPμ to sites of cell-cell contact in GM7372 cells.** GM7372 cells expressing the empty pWZL-hygro vector, T7 epitope-tagged PTPμWT, PTPμΔIg, or PTPμΔE were grown to confluence, fixed, and co-stained with antibodies to the T7 epitope and VE-cadherin (*cad*). *Green* (*left panels*) and *red* (*right panels*) channels for each field are shown side by side. *Arrowheads* indicate examples of PTPμ-T7 and VE-cadherin localization at sites of cell-cell contact. Nuclear staining is seen in all samples stained with the anti-T7 epitope antibody, including cells expressing the empty pWZL vector, and therefore is not representative of PTPμ-T7 localization. *Scale bar* = 10 μm.

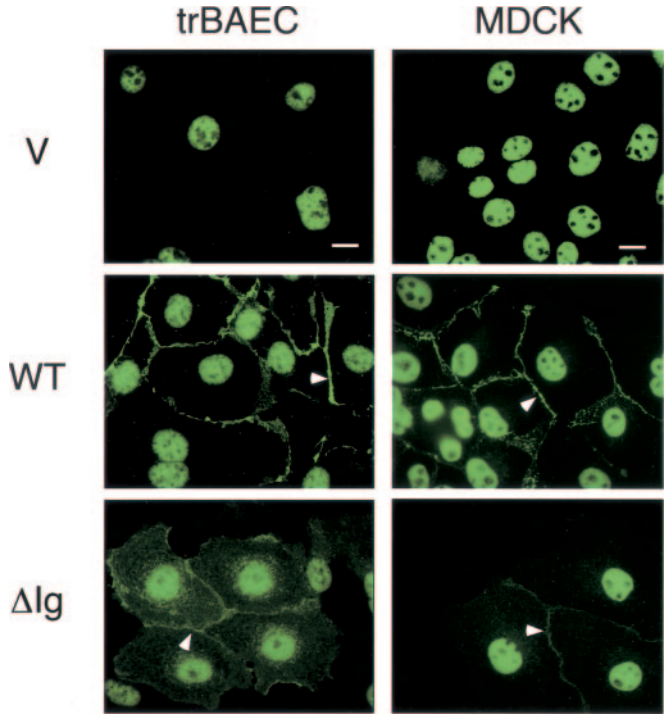

FIG. 4. **Localization of ectopic PTPμ in trBAEC and MDCK cells.** Stable lines of trBAEC and MDCK cells expressing the empty pWZL-hygro vector (*V*), T7 epitope-tagged PTPμWT, or PTPμΔIg constructs were grown to confluence, fixed, and stained with the anti-T7 epitope antibody. Nuclear staining is seen in all samples, including cells expressing the empty pWZL vector, and therefore is not representative of PTPμ-T7 localization. *Arrowheads* indicate examples of PTPμ-T7 localization at areas of cell-cell contact (PTPμWT and PTPμΔIg). *Scale bars* = 10 μm.

homophilic binding may be responsible for localization of PTPμ to cell-cell contacts (10, 11). To test this idea in a cellular context, GM7372 cells expressing T7 epitope-tagged PTPμ mutants were analyzed by indirect immunofluorescence with the anti-T7 epitope antibody to determine the subcellular localization of the phosphatase. Full-length PTPμ-WTT7 localized to cell-cell contacts as indicated by co-localization with VE-cadherin (Fig. 3, *WT panels*). Deletion of the Ig domain, containing the homophilic binding site, greatly reduced the localization of PTPμ to cell-cell contacts (Fig. 3, *ΔIg panels*), resulting in a dispersed pattern consistent with expression at the cell surface. Therefore, the Ig domain, which contains the homophilic binding site (10), is a major determinant for localization to cell-cell contacts, suggesting that homophilic binding is important for this localization. Deletion of the entire E-subunit, containing most of the extracellular domain, completely eliminated localization of PTPμ to cell-cell contacts (Fig. 3, *ΔE panels*), suggesting that this region may contain sequences in addition to the Ig domain that play a part in this localization. A role has been proposed for the MAM domain in homophilic binding (11); however, we were unable to determine whether the MAM domain may contribute to the localization of PTPμ because constructs with a deletion of this domain could not be stably expressed at levels comparable with the other mutants (data not shown). This is consistent with studies of the metalloprotease meprin A, which have suggested that the MAM domain may be critical for protein stability (34).

To verify that the localization of PTPμΔIg in GM7372 cells is a property of the phosphatase and not a phenomenon unique to these cells, we examined the localization the PTPμ deletion constructs in two additional cell types, a transformed endothelial cell line trBAEC and MDCK epithelial cells, the latter being a well established model for studying cell-cell adhesion. In trBAEC and MDCK cells, as seen in GM7372 cells, deletion of the Ig domain resulted in reduced localization to cell-cell contacts and a more dispersed distribution over the cell compared with the WT protein (Fig. 4). These results confirm that the Ig domain is a major determinant for the localization of PTPμ to cell-cell contacts in multiple cell types.

The PTPμΔIg Protein Is Present at the Cell Surface—As described above, deletion of the Ig domain led to a widespread distribution of PTPμ over what appeared to be the cell surface. To confirm that the PTPμΔIg protein was present at the cell surface, we used the extracellular domain-specific antibody BK2 to stain GM7372 cells that had not been permeabilized prior to antibody staining. PTPμWT was detected primarily at cell-cell contacts in intact non-permeabilized cells, whereas PTPμΔIg was dispersed over the surface of the cell (Fig. 5). Staining of permeabilized cells revealed additional localization of both PTPμWT and PTPμΔIg in a perinuclear region (Fig. 5) as described for the endogenous protein (Fig. 1). We were unable to determine whether PTPμΔE can reach the cell surface, as it did not react with the available antibodies directed against the extracellular region of PTPμ.

To analyze the localization of the mutant PTPμ proteins in

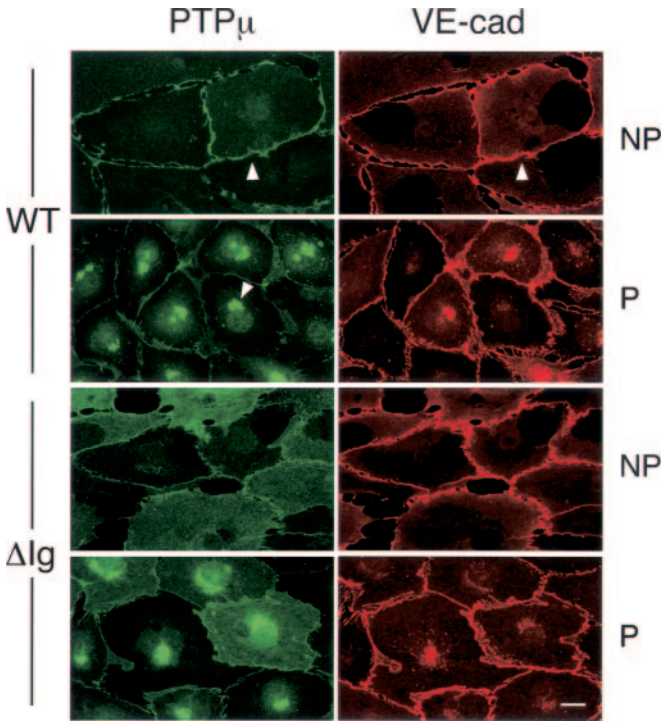

FIG. 5. **PTPμΔIg is present at the cell surface of GM7372 cells.** GM7372 cells expressing PTPμWT or PTPμΔIg were grown to confluence and fixed. Cells were either permeabilized as described under "Experimental Procedures" (*P*) or left intact (*NP*) and then co-stained with anti-PTPμ E-subunit antibody BK2 and anti-VE-cadherin antibody 45C6 (*VE-cad*). *Green* (*left panels*) and *red* (*right panels*) channels for each field are shown side by side. PTPμWT is seen at cell-cell contacts of non-permeabilized cells (*first row*, *arrowheads*), whereas in permeabilized cells, additional staining is observed in an intracellular perinuclear region (*second row*, *arrowhead*). In cells expressing detectable PTPμΔIg, the surface-exposed mutant protein can be seen as a diffuse staining pattern in non-permeabilized cells (*third row*) and permeabilized cells (*fourth row*). Staining at cell-cell contacts in the PTPμΔIg samples can be attributed, in part, to endogenous PTPμ. Samples were viewed with a ×40 objective lens. *Scale bar* = 10 μm.

further detail, we examined MDCK cells, which, in contrast to GM7372 endothelial cells, form a monolayer in culture with sufficient depth to visualize cell morphology in three dimensions using confocal microscopy. Cross-section imaging of MDCK cells expressing full-length PTPμWT and PTPμWTΔD2, a mutant lacking the membrane distal catalytic domain, stained with an antibody directed against the P-subunit of PTPμ, indicated that these proteins, which contain an intact E-subunit, were found concentrated along most of the lateral cell-cell contacts (Fig. 6). Co-staining with antibodies to the tight junction protein ZO-1, a marker for the apical junction, showed that PTPμWT was absent from the apical terminal portion of the lateral surface (data not shown). In contrast, the PTPμΔIg protein was seen in the lateral junction and on the apical and basal surfaces of the monolayer. This diffuse surface staining of PTPμΔIg observed in GM7372 cells was also seen in an image of MDCK cells from a section in the *x-y* plane (Fig. 6, *right ΔIg panel*). In contrast to PTPμΔIg, the PTPμΔE protein, with the entire E-subunit deleted, was concentrated in heterogeneous membrane structures throughout the cytoplasm and absent from lateral cell-cell contacts and the apical surface. Therefore, the loss of the Ig domain resulted in reduced cell-cell contact localization and diffuse surface expression of the PTPμ mutant in both GM7372 endothelial cells and MDCK cells.

Deletion of the Ig Domain Affects Localization of PTPμ in Subconfluent Cells—In contrast to what has been proposed for PTPμWT (11), the distribution of PTPμΔIg in confluent cells (Figs. 3–6) suggested that stable surface expression of this mutant can be maintained independently of localization to cell-cell contacts. Therefore, we examined subconfluent GM7372 cells, which lack cell-cell contacts, to determine whether PTPμΔIg was, in contrast to the WT protein (Fig. 1), stably expressed at the cell surface. Staining of non-permeabilized cells revealed that PTPμΔIg was expressed over the surface of subconfluent cells with a high concentration seen at certain regions of the cell periphery (Fig. 7). In contrast, little surface staining could be observed in cells expressing PTPμWT (Fig. 7). Permeabilization of cells prior to staining revealed the intracellular localization of both PTPμWT and PTPμΔIg (Fig.

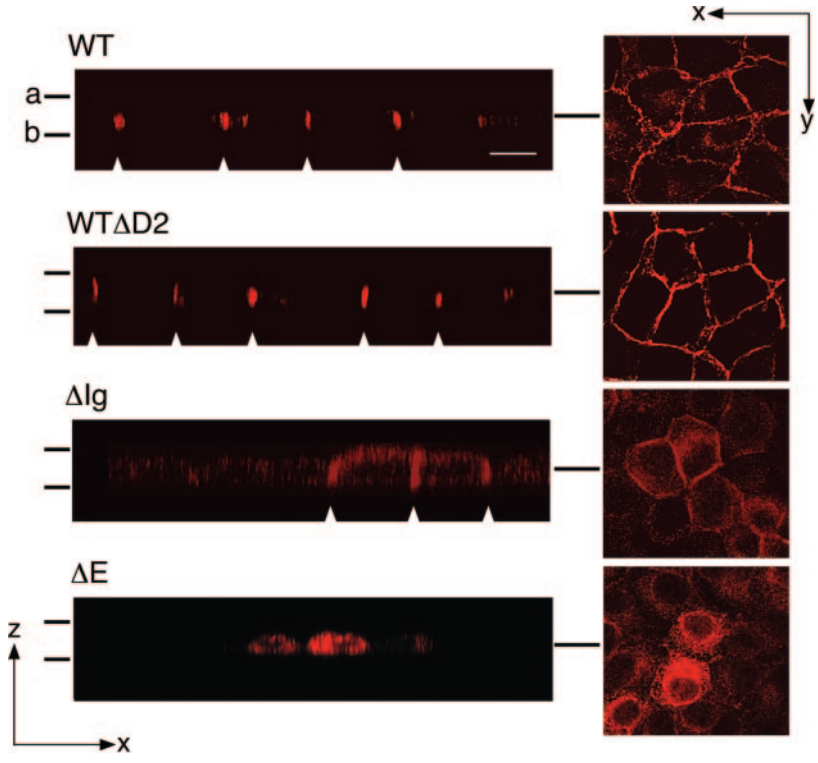

FIG. 6. **PTPμΔIg localizes to apical and basal surfaces of MDCK cells.** MDCK cells expressing the indicated PTPμ-T7 constructs (PTPμWT, PTPμWTΔD2, PTPμΔIg, and PTPμΔE) were grown to 100% confluence, fixed, and stained with anti-PTPμ antibody SK7. Antibody SK7 does not react significantly with parental MDCK cells. Samples were imaged in the *x-z* axis (*left panels*, axis shown at lower left) using a Zeiss LSM550 confocal microscope with a ×100 objective lens. Localization of expressed PTPμ at lateral cell-cell contacts is indicated by *arrowheads*. The position of the apical surface (*a*) of the cell monolayer is at the top of each panel, and the position of the basal surface (*b*) is at the bottom, as indicated by the *lines*. Images from 0.4-μm sections in the *x-y* plane are shown (*right panels*) with the approximate position of the plane in the *z* dimension indicated by a *solid line* to the corresponding *x-z* image. *Scale bar* = 10 μm.

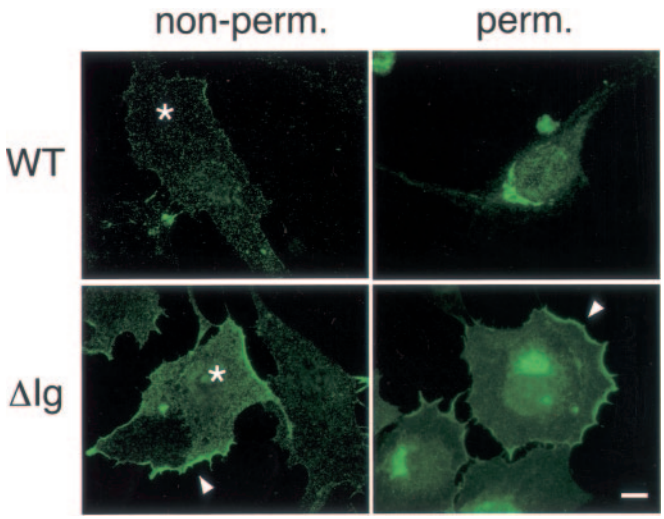

FIG. 7. **The PTPμΔIg protein is present at the surface of subconfluent GM7372 cells.** GM7372 cells expressing either PTPμWT-T7 or PTPμΔIg were grown to confluence and fixed. Cells were either permeabilized as described under "Experimental Procedures" (*perm.*) or left intact (*non-perm.*) and then stained with anti E-subunit antibody BK2. *Asterisks* indicate a PTPμWT-expressing cell displaying little detectable PTPμ surface expression and a PTPμΔIg-expressing cell showing elevated levels of PTPμ surface expression with localized concentration at the periphery (*arrowheads*). *Scale bar* = 10 μm.

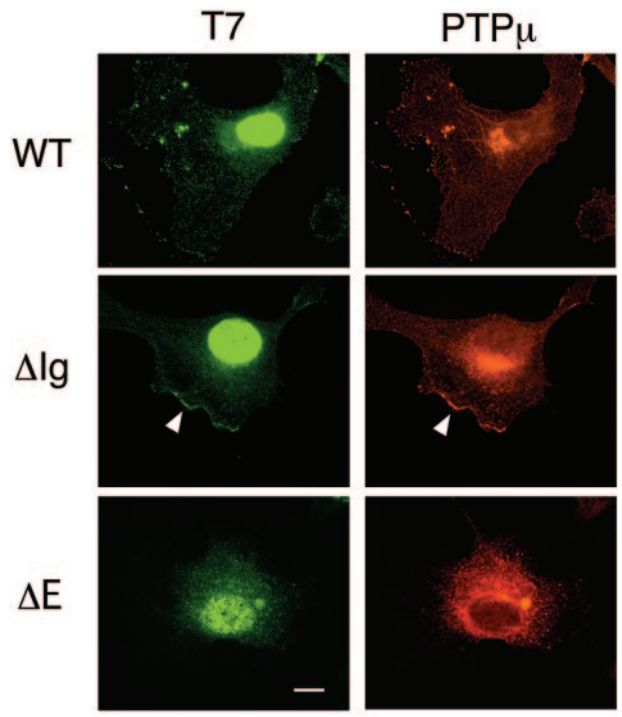

FIG. 8. **Localization of PTPμ-T7 proteins in subconfluent GM7372 cells.** GM7372 cells expressing PTPμWT-T7, PTPμΔIg, or PTPμΔE were plated on glass coverslips, fixed, and co-stained with the anti-T7 epitope antibody (*green*) and anti-PTPμ P-subunit antibody SK7 (*red*). *Green* (*left panels*) and *red* (*right panels*) channels for each field are shown side by side. *Arrowheads* indicate unique localization of the PTPμΔIg protein seen in 68 of 107 cells examined. Shown is an example of a typical PTPμWT-expressing cell exhibiting no peripheral localization for PTPμ. *Scale bar* = 10 μm.

7), as observed for endogenous PTPμ (Fig. 1*C*).

To confirm the presence of epitope-tagged PTPμΔIg at the cell periphery, we stained permeabilized cells with the anti-T7 epitope antibody in combination with anti-P-subunit antibody SK7. In 68 of 107 cells (64%) observed, PTPμΔIg showed a striking pattern of expression at regions of the cell periphery (Fig. 8), whereas peripheral localization of PTPμWT was seen in only 6 of 102 cells (6%). Deletion of the entire E-subunit eliminated the peripheral localization seen with the PTPμΔIg mutant, indicating that some features of the extracellular domain are required for targeting PTPμΔIg to the cell periphery (Fig. 8). Therefore, deletion of the Ig domain allowed PTPμ to concentrate at the cell periphery in subconfluent cells by a mechanism requiring some other elements of the E-subunit.

Ectopic Expression of PTPμ Induces Alterations in Focal Adhesion and Actin Cytoskeleton Morphology—The aberrant localization of PTPμΔIg in subconfluent GM7372 cells suggested that this protein may modulate events that occur at the cell periphery such as the formation of nascent cell-matrix junctions. Consistent with this idea, the morphology of focal adhesions and cytoskeleton components was affected by overexpression of PTPμΔIg in sparse cultures of GM7372 cells. Vector control cells (Fig. 9, *vector panels*) showed the characteristic punctate pattern of vinculin-containing focal adhesions (1). In cultures expressing PTPμΔIg, many cells displayed a broad region of vinculin staining that co-localized with the phosphatase at the cell periphery (Fig. 9, *ΔIg panels*, *arrowheads*).

The presence of PTPμΔIg at the cell periphery correlated with the redistribution of phosphotyrosine proteins from discrete punctate areas, as seen in vector control cells (Fig. 9, *vector panels*), to continuous broad regions of staining that coincided with the mutant PTP at the cell periphery (*ΔIg panels*, *arrowheads*). Again, the changes in phosphotyrosine localization in PTPμWT cells were minor compared with those seen with PTPμΔIg (Fig. 9). These results, in combination with the redistribution of vinculin, suggest that the aberrant localization of PTPμΔIg results in specific changes that affect the formation of focal contacts at the cell periphery, rather than the large-scale dephosphorylation of phosphotyrosine proteins in general. The specific PTP activities of PTPμΔIg and PTPμWT immunoprecipitated from lysates of GM7372 cells were similar (data not shown), suggesting that the effects caused by PTPμΔIg correlate with the unique localization of this mutant and are not caused by a change in activity.

Further analysis by immunoblotting lysates with anti-phosphotyrosine antibodies did not reveal consistent changes in the pattern of protein tyrosine phosphorylation in response to expression of PTPμWT or PTPμΔIg, reinforcing the idea that the ectopic expression of the phosphatase causes limited changes in tyrosine phosphorylation. We tested several potential targets of PTPμ, including β-catenin and $p120^{ctn}$ (35), as well as the major focal adhesion phosphotyrosine proteins focal adhesion kinase, c-Src, paxillin, and $p130^{cas}$, as suggested by the localization of PTPμΔIg. In the presence of ectopic PTPμWT or PTPμΔIg, we did not detect consistent changes in the state of tyrosine phosphorylation of these proteins by immunoblotting with anti-phosphotyrosine antibodies or phospho-specific antibodies.

To examine further the state of cell-matrix contacts, we visualized the distribution of the focal adhesion protein paxillin (1). In cells expressing empty vector or PTPμWT, paxillin was visualized in a punctate staining pattern at regions at the cell-matrix interface characteristic of focal adhesions (Fig. 10). The sizes of the punctate regions observed in WT cells were not as uniformly large as those of the vector control cells. Cells expressing PTPμΔIg exhibited a diffuse pattern of paxillin localization with some punctate staining at the cell periphery (Fig. 10). Similarly, PTPμΔIg cells displayed numerous tensin-containing contacts, but they were not as large as those seen with cells expressing empty vector or PTPμWT (data not shown). In light of the interdependence of focal adhesions and the actin cytoskeleton, the morphology of F-actin was also

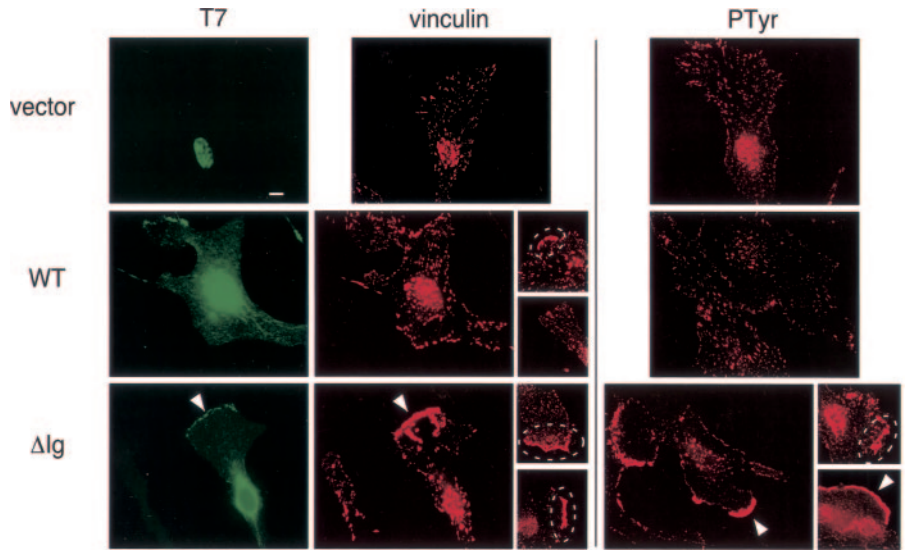

FIG. 9. **Aberrant localization of vinculin and phosphotyrosine proteins at the cell periphery of GM7372 cells expressing PTPμΔIg.** GM7372 cells expressing PTPμ constructs were plated on glass coverslips, fixed, and co-stained with the anti-T7 epitope (*green*) and anti-vinculin (*red*) antibodies or stained with the anti-phosphotyrosine antibody (*PTyr*; *red*). The constructs expressed are indicated to the left. The *small frames* show additional examples from the PTPμWT and PTPμΔIg samples with focus on the cell periphery. *Arrowheads* and *dashed ovals* point out the unique patterns of PTPμΔIg, vinculin, and phosphotyrosine proteins. *Scale bar* = 10 μm.

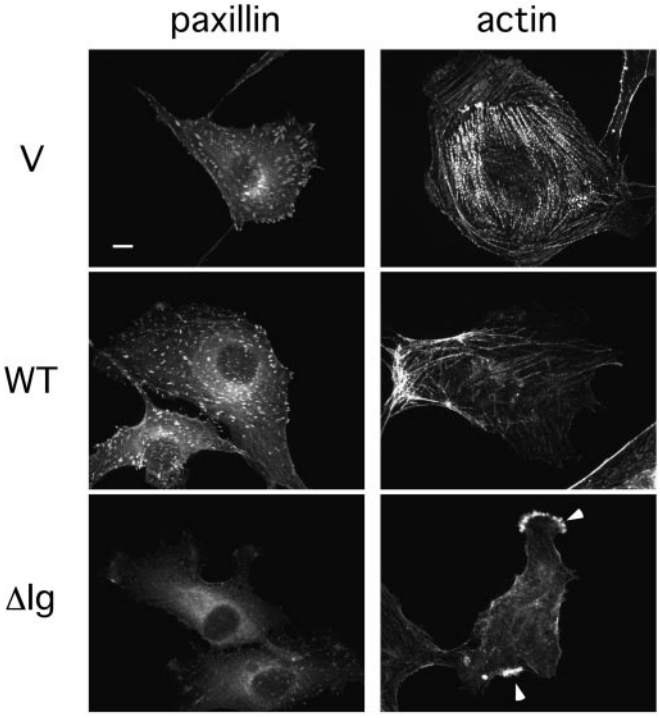

FIG. 10. **Expression of PTPμΔIg affects formation of focal adhesions and actin stress fibers in subconfluent GM7372.** GM7372 cells expressing the empty pWZL-hygro vector (*V*), PTPμWT, or PTPμΔIg were plated on glass coverslips, fixed, and stained with either the anti-paxillin antibody or Alexa 594-labeled phalloidin to detect F-actin (*actin*). Irregular localization of actin in PTPμΔIg-expressing cells is indicated by *arrowheads*. *Scale bar* = 10 μm.

examined. PTPμΔIg cells exhibited poorly defined actin-based stress fibers; instead, F-actin was found at restricted loci at the cell periphery (Fig. 10). Cells expressing empty vector showed well formed stress fibers, whereas PTPμWT-expressing cells displayed short stress fibers with numerous branches (Fig. 10, *V* and *WT panels*).

Expression of PTPμ Constructs Impairs Survival of GM7372 Cells—The defects in cell-matrix junction morphology might be expected to impair cell growth and/or survival (36, 37). Furthermore, we would anticipate that these effects would be more pronounced at low cell density, when cells are more dependent upon signals generated from cell-matrix junctions for survival, and could explain the difficulties in generating stable clones of GM7327 cells expressing PTPμ. To test this hypothesis, GM7372 cells infected with recombinant retrovirus encoding pWZL/PTPμ mutants were plated at various densities from ~50% confluence (1×10^4 cells/cm^2) to ~5% confluence (0.11×10^4 cells/cm^2) and incubated for 15 days, and the cell number was estimated by staining with crystal violet. Comparison of cells expressing empty vector with those expressing different PTPμ constructs indicated that at each given plating density, expression of PTPμΔIg had the greatest inhibitory effect on cell number compared with the PTPμWT and PTPμΔE proteins (Fig. 11*A*). The four cell lines exhibited similar rates of proliferation represented by the percentage of cells progressing through the cell cycle as indicated by the incorporation of BrdUrd (Fig. 11*B*). However, PTPμΔIg-expressing cultures exhibited increased levels of apoptosis compared with the other cell lines (Fig. 11*B*). As cells complete apoptosis, they dissociate from the culture dish and are not counted in the assay we used. As a result, the percentage of apoptotic cells presented in Fig. 11 likely under-represents the rate of apoptosis of the cultures. Therefore, consistent with the changes in focal adhesions and the actin cytoskeleton, expression of PTPμΔIg reduced the survival of GM7372 cells.

DISCUSSION

The precise consequence of ligand binding is not understood for most RPTPs, but the structural relationship of enzymes such as PTPμ to cell adhesion molecules suggests that one purpose of the extracellular segment may be to position the phosphatase at sites of cell adhesion. In this regard, it has been suggested that homophilic binding, the engagement of a PTPμ molecule on one cell by another PTPμ molecule on an apposing cell, directs localization of PTPμ to sites of cell-cell contact. At this location, PTPμ is thought to regulate the cell junction complexes that control cell-cell adhesion (11, 15). We examined the role of the conserved Ig domain, which contains the homophilic binding site, in regulating PTPμ in cultured cells. Recent studies have conveyed the importance of Ig domains in the extracellular segments of RPTP-LAR and PTPσ, which are in a different structural class from PTPμ. In *Drosophila*, the three Ig domains of PTP-LAR have been shown to be important for survival (38). The N-terminal Ig domain of PTPσ mediates binding to heparin sulfate proteoglycans and may be critical in targeting the phosphatase to sites of cell-matrix interaction (39). Mutations in the Ig domain of the *Caenorhabditis elegans* RPTP CLR-1 compromise the ability of the phosphatase to control axonal guidance (40). Our results indicate that the Ig

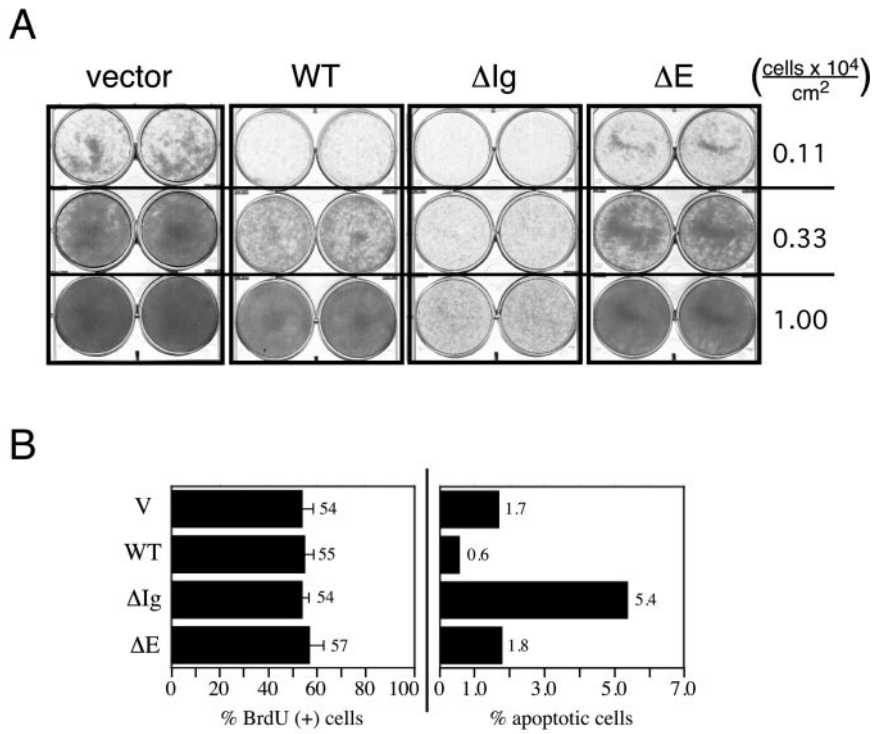

FIG. 11. **Expression of PTPμ constructs in GM7372 cells results in reduced cell survival.** *A*, GM7372 cells infected with recombinant retrovirus encoding PTPμWT, PTPμΔIg, or PTPμΔE or the empty pWZL-hygro vector were plated at 1.0, 0.33, and 0.11×10^4 cells/cm^2 in duplicate and grown in selective medium for 15 days. Culture density was visualized by staining with crystal violet. *B*, *left panel*, GM7372 cells expressing the indicated PTPμ proteins or the empty vector control (*V*) were assayed for proliferation by measuring the incorporation of BrdUrd into chromatin as described under "Experimental Procedures." The *solid bars* and *numbers* represent the percentage of cells that incorporate BrdUrd (*BrdU (+)*), with each bar representing the mean ± S.E. of three cell counts. *Right panel*, cells undergoing apoptosis were identified and counted as described under "Experimental Procedures." The *solid bars* and *numbers* represent the percentage of apoptotic cells for each culture.

domain of PTPμ not only is involved in localization of the enzyme to cell-cell contacts, but may also control localization in the absence of cell-cell contact.

To explore the function of the Ig domain in PTPμ, we generated a construct, termed PTPμΔIg, in which this domain had been deleted. The integrity of this mutant protein is supported by several observations. As in the case with the wild-type enzyme, the mutant protein was processed normally into a P-subunit (containing the intracellular PTP domains), which was associated with the E-subunit, here comprising the mutated extracellular segment. In addition, the enzymatic activity and half-life of PTPμΔIg were unaffected compared with those of the wild-type enzyme. Furthermore, the data in Fig. 3, showing that regions of the E-subunit other than the Ig domain contribute to the residual localization of PTPμΔIg to cell-cell contacts, also suggest that some function is retained in either the MAM domain or fibronectin type III repeats when the Ig domain is deleted. In contrast to what has been proposed for PTPμWT (11), the PTPμΔIg protein, which is not localized to sites of cell-cell contact, was observed at the cell surface. As outlined in Fig. 12, PTPμ is thought to cycle to and from the plasma membrane in subconfluent cells through membrane structures in the perinuclear region of the cell (11, 15), thereby limiting its access to other cell compartments, including cell-matrix junctions. When culture density increases and cells make contact, homophilic binding would restrict PTPμ to sites of cell-cell contact where the ligand, another PTPμ molecule, would be available on an apposing cell. With the loss of the Ig domain, the normal cycling of PTPμ was disrupted such that the PTPμΔIg protein was widely distributed at the cell surface and concentrated at the cell periphery, where it could interact with cell-matrix junctions.

Although our data illustrate that the Ig domain is critical to the control of PTPμ localization in both confluent and subconfluent cells, its mechanism of action in each case may be different. One possibility is that the extracellular segment, including the Ig domain, mediates a combination of *trans*-homophilic (apposing cell) and *cis*-homophilic (with PTPμ on the same cell) interactions, which may regulate localization of PTPμ either in the presence or absence of cell-cell contact. There is evidence that some cell adhesion molecules such as cadherin and L1CAM participate in combinations of *cis*- and *trans*-homophilic interactions often involving multiple conserved domains, including Ig domains (41, 42). One function for the *cis*-interactions is to mediate the formation of multimeric receptor complexes that increase the avidity of the *trans*-interactions, thereby strengthening cell-cell adhesion complexes (41). Furthermore, *cis*-interactions may also affect the transport of adhesion proteins to and from the cell surface and, as a result, may control localization in the absence of cell adhesion (42). In light of these precedents, it is possible that elements of the PTPμ extracellular domain may participate in both *trans*- and *cis*-homophilic interactions, controlling localization of the phosphatase either in the presence or absence of cell-cell contact.

Previous studies have demonstrated that PTPμ associates with classical cadherins such as E-cadherin, N-cadherin, and cadherin-4 (43) and that PTPμ can modulate cell adhesion to culture surfaces coated with N- or E-cadherin (44, 45). However, PTPμΔIg did not induce major changes in the localization of VE-cadherin, suggesting that the integrity of cell-cell contacts was maintained (Figs. 3 and 5). Instead, the consequences of PTPμΔIg expression were most apparent in subconfluent cells in the absence of cadherin-dependent cell-cell adhesion and suggested that this mutant acts on a component of cell-matrix junctions or the associated actin cytoskeleton. Considering that many potential targets of PTPμ in cell-cell junctions are also found in cell-matrix junctions, the effects caused by the Ig domain deletion mutant may be a result of the mislocalized phosphatase acting on a normal PTPμ substrate in the wrong context, that of the focal adhesion in subconfluent cells. We were unable to detect changes in the global pattern of tyrosine phosphorylation, implying that the expressed forms of PTPμ did not act in a broad, nonspecific manner, but instead exhibited selectivity in action, leading to the effects on focal adhesions and cell survival. Although p120^{ctn}, a phosphotyrosine protein that may function in both cell-cell and cell-matrix adhesions, could be such a substrate (35, 46), we did not detect consistent changes in the tyrosine phosphorylation of this or other potential substrates following expression of either the PTPμWT or PTPμΔIg protein.

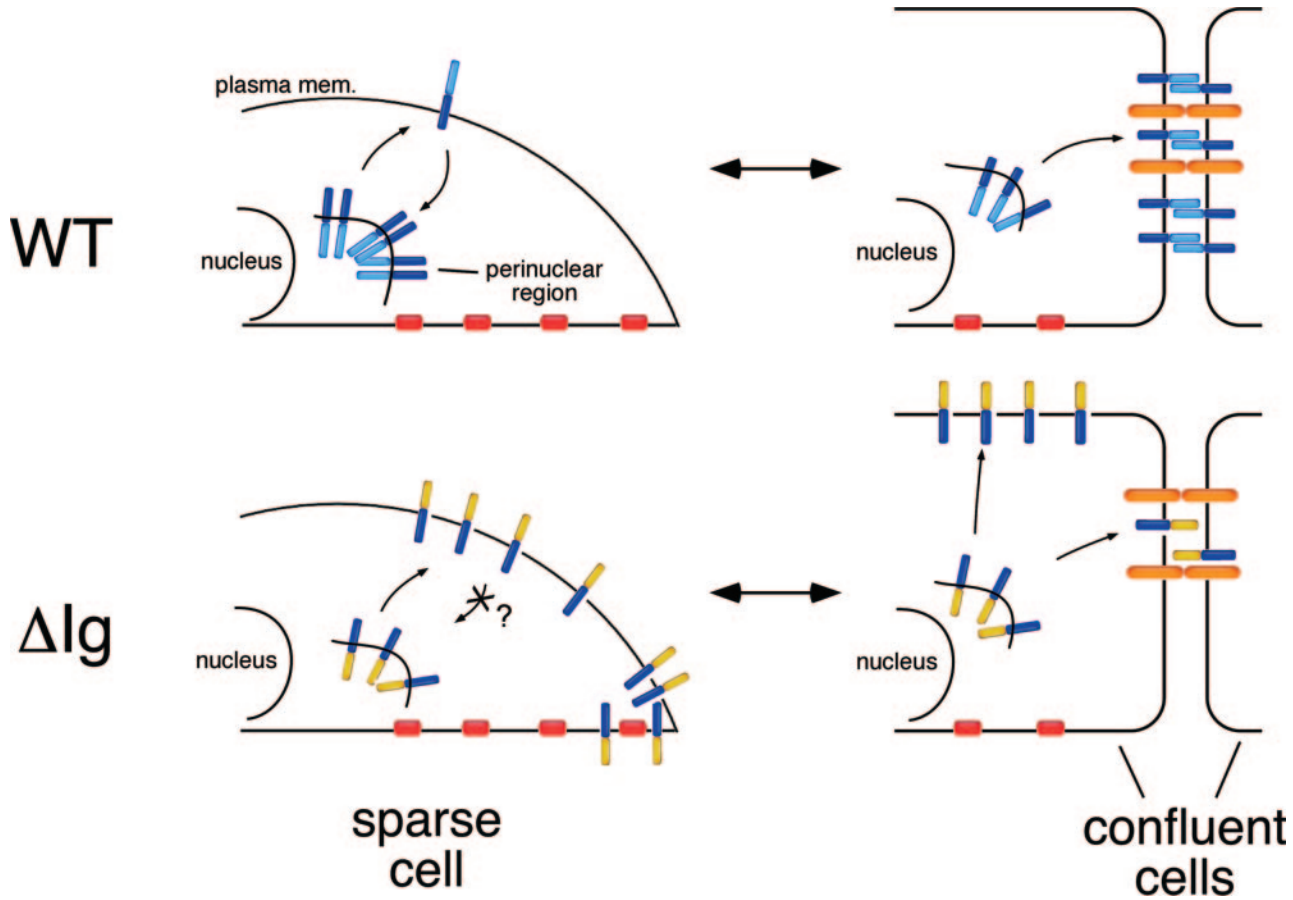

FIG. 12. **The Ig domain is required for appropriate localization of PTPμ.** The diagram illustrates the distribution of PTPμWT in sparse and confluent cells, including the effects of deletion of the extracellular Ig domain (ΔIg). PTPμWT is shown with the E-subunit in *light blue* and the P-subunit in *dark blue*, and the E-subunit of PTPμΔIg is shown in *yellow*. The plasma membrane (*mem.*) and nucleus are indicated. The perinuclear localization of PTPμ is shown to the right of the nucleus. Cadherin-containing cell-cell junctions are indicated by the *orange bars* that bridge two apposing confluent cells, and cell-matrix junctions are shown in *red* at the basal surface of the cell. It has been proposed that stable surface expression of PTPμ is dependent upon its localization to sites of cell-cell contact as directed by homophilic binding to another PTPμ molecule on an apposing cell. Deletion of the Ig domain disrupts the normal localization of PTPμ, significantly reducing the amount PTPμΔIg at regions of cell-cell contact and allowing for the stable surface expression of PTPμΔIg. One possibility is that the Ig domain is required for the internalization of PTPμ (*arrow* from the plasma membrane for PTPμWT) that occurs when homophilic binding is not possible, and therefore, PTPμΔIg remains at the surface, allowing for aberrant localization to the cell periphery in the area occupied by cell-matrix junctions.

In defining a role for the Ig domain in regulating PTPμ, we have illustrated the importance of this region in positioning the phosphatase at its proposed site of action, cell-cell junctions. In addition, this analysis has also brought to light the importance of the Ig domain in restricting PTPμ localization to prevent it from acting on improper targets. In subconfluent GM7372 cells, which normally maintain a low level of endogenous PTPμ, increasing the amount of the phosphatase by ectopic expression of the wild-type enzyme impaired cell survival. However, expression of the PTPμΔIg mutant exerted more severe effects on cell survival as well as changes in focal adhesion and cytoskeleton morphology. These effects correlated with the atypical localization of this mutant, rather than the level of protein expression or phosphatase activity. Our analysis therefore highlights the importance of regulation of the localization of PTPμ in controlling the function of the enzyme and the maintenance of normal cell physiology.

Acknowledgments—We thank K. Pennino, M. Daddario, and M. Ye for technical assistance; S. Hearn for help with confocal microscopy; G. J. Hannon and D. Conklin for providing LiNX-A cells; and A. Piccini, D. Buckley, and S. Muthuswamy for advice on the manuscript.

REFERENCES

1. Zamir, E., and Geiger, B. (2001) *J. Cell Sci.* **114,** 3583–3590
2. Daniel, J. M., and Reynolds, A. B. (1997) *BioEssays* **19,** 883–891
3. Garton, A. J., and Tonks, N. K. (1999) *J. Biol. Chem.* **274,** 3811–3818
4. Harder, K. W., Moller, N. P., Peacock, J. W., and Jirik, F. R. (1998) *J. Biol. Chem.* **273,** 31890–31900
5. Su, J., Muranjan, M., and Sap, J. (1999) *Curr. Biol.* **9,** 505–511
6. Thomas, S. M., and Brugge, J. S. (1997) *Annu. Rev. Cell Dev. Biol.* **13,** 513–609
7. Brady-Kalnay, S. M., and Tonks, N. K. (1995) *Curr. Opin. Cell Biol.* **7,** 650–657
8. Beltran, P. J., and Bixby, J. L. (2003) *Front. Biosci.* **8,** D87–D99
9. Larsen, M., Tremblay, M. L., and Yamada, K. M. (2003) *Nat. Rev. Mol. Cell. Biol.* **4,** 700–711
10. Brady-Kalnay, S. M., and Tonks, N. K. (1994) *J. Biol. Chem.* **269,** 28472–28477
11. Gebbink, M. F., Zondag, G. C., Koningstein, G. M., Feiken, E., Wubbolts, R. W., and Moolenaar, W. H. (1995) *J. Cell Biol.* **131,** 251–260
12. Beckmann, G., and Bork, P. (1993) *Trends Biochem. Sci.* **18,** 40–41
13. Brady-Kalnay, S. M., Flint, A. J., and Tonks, N. K. (1993) *J. Cell Biol.* **122,** 961–972
14. Gebbink, M. F., Zondag, G. C., Wubbolts, R. W., Beijersbergen, R. L., van Etten, I., and Moolenaar, W. H. (1993) *J. Biol. Chem.* **268,** 16101–16104
15. Brady-Kalnay, S. M., Rimm, D. L., and Tonks, N. K. (1995) *J. Cell Biol.* **130,** 977–986
16. Ostman, A., Yang, Q., and Tonks, N. K. (1994) *Proc. Natl. Acad. Sci. U. S. A.* **91,** 9680–9684
17. Symons, J. R., LeVea, C. M., and Mooney, R. A. (2002) *Biochem. J.* **365,** 513–519
18. Gaits, F., Li, R. Y., Ragab, A., Ragab-Thomas, J. M., and Chap, H. (1995) *Biochem. J.* **311,** 97–103
19. Bianchi, C., Sellke, F. W., Del Vecchio, R. L., Tonks, N. K., and Neel, B. G. (1999) *Exp. Cell Res.* **248,** 329–338
20. Tonks, N. K., and Neel, B. G. (2001) *Curr. Opin. Cell Biol.* **13,** 182–195
21. Bilwes, A. M., den Hertog, J., Hunter, T., and Noel, J. P. (1996) *Nature* **382,** 555–559
22. Majeti, R., Bilwes, A. M., Noel, J. P., Hunter, T., and Weiss, A. (1998) *Science* **279,** 88–91
23. Jiang, G., den Hertog, J., Su, J., Noel, J., Sap, J., and Hunter, T. (1999) *Nature* **401,** 606–610
24. Hoffmann, K. M., Tonks, N. K., and Barford, D. (1997) *J. Biol. Chem.* **272,** 27505–27508

25. Nam, H. J., Poy, F., Krueger, N. X., Saito, H., and Frederick, C. A. (1999) *Cell* **97,** 449–457
26. Aicher, B., Lerch, M. M., Muller, T., Schilling, J., and Ullrich, A. (1997) *J. Cell Biol.* **138,** 681–696
27. Serra-Pages, C., Kedersha, N. L., Fazikas, L., Medley, Q., Debant, A., and Streuli, M. (1995) *EMBO J.* **14,** 2827–2838
28. Wang, J., and Bixby, J. L. (1999) *Mol. Cell. Neurosci.* **14,** 370–384
29. Grinspan, J. B., Mueller, S. N., and Levine, E. M. (1983) *J. Cell. Physiol.* **114,** 328–338
30. Lutz-Freyermuth, C., Query, C. C., and Keene, J. D. (1990) *Proc. Natl. Acad. Sci. U. S. A.* **87,** 6393–6397
31. Gebbink, M. F., van Etten, I., Hateboer, G., Suijkerbuijk, R., Beijersbergen, R. L., Geurts, van Kessel, A. G., and Moolenaar, W. H. (1991) *FEBS Lett.* **290,** 123–130
32. Wang, J., Xie, L. Y., Allan, S., Beach, D., and Hannon, G. J. (1998) *Genes Dev.* **12,** 1769–1774
33. Garton, A. J., Burnham, M. R., Bouton, A. H., and Tonks, N. K. (1997) *Oncogene* **15,** 877–885
34. Tsukuba, T., and Bond, J. S. (1998) *J. Biol. Chem.* **273,** 35260–35267
35. Zondag, G. C., Reynolds, A. B., and Moolenaar, W. H. (2000) *J. Biol. Chem.* **275,** 11264–11269
36. Re, F., Zanetti, A., Sironi, M., Polentarutti, N., Lanfrancone, L., Dejana, E., and Colotta, F. (1994) *J. Cell Biol.* **127,** 537–546
37. Frisch, S. M., and Francis, H. (1994) *J. Cell Biol.* **124,** 619–626
38. Krueger, N. X., Reddy, R. S., Johnson, K., Bateman, J., Kaufmann, N., Scalice, D., Van Vactor, D., and Saito, H. (2003) *Mol. Cell. Biol.* **23,** 6909–6921
39. Aricescu, A. R., McKinnell, I. W., Halfter, W., and Stoker, A. W. (2002) *Mol. Cell. Biol.* **22,** 1881–1892
40. Chang, C., Yu, T. W., Bargmann, C. I., and Tessier-Lavigne, M. (2004) *Science* **305,** 103–106
41. Boggon, T. J., Murray, J., Chappuis-Flament, S., Wong, E., Gumbiner, B. M., and Shapiro, L. (2002) *Science* **296,** 1308–1313
42. Haspel, J., and Grumet, M. (2003) *Front. Biosci.* **8,** s1210–s1225
43. Brady-Kalnay, S. M., Mourton, T., Nixon, J. P., Pietz, G. E., Kinch, M., Chen, H., Brackenbury, R., Rimm, D. L., Del Vecchio, R. L., and Tonks, N. K. (1998) *J. Cell Biol.* **141,** 287–296
44. Burden-Gulley, S. M., and Brady-Kalnay, S. M. (1999) *J. Cell Biol.* **144,** 1323–1336
45. Hellberg, C. B., Burden-Gulley, S. M., Pietz, G. E., and Brady-Kalnay, S. M. (2002) *J. Biol. Chem.* **277,** 11165–11173
46. Anastasiadis, P. Z., and Reynolds, A. B. (2001) *Curr. Opin. Cell Biol.* **13,** 604–610